A role of anterior cingulate cortex in the emergence of worker–parasite relationship

Soyoun Ahn[a,1], Yujeong Kang[b,1], Jong Won Lee[b,1], Se Jin Jeong[c,1], Yoo Jin Lee[c], Soomin Lee[c], Jeongyeon Kim[c], Ja Wook Koo[c,d,2], Jeansok J. Kim[e,f,2], and Min Whan Jung[a,b,2]

[a]Department of Biological Sciences, Korea Advanced Institute of Science and Technology, Daejeon 34141, Korea; [b]Center for Synaptic Brain Dysfunctions, Institute for Basic Science, Daejeon 34141, Korea; [c]Emotion, Cognition & Behavior Research Group, Korea Brain Research Institute, Daegu 41062, Korea; [d]Department of Brain and Cognitive Sciences, Daegu Gyeongbuk Institute of Science and Technology, Daegu 42988, Korea; [e]Department of Psychology, University of Washington, Seattle, WA 98195-1525; and [f]Program in Neuroscience, University of Washington, Seattle, WA 98195-1525

Edited by Gene E. Robinson, University of Illinois at Urbana–Champaign, Urbana, IL, and approved October 29, 2021 (received for review June 22, 2021)

We studied the brain mechanisms underlying action selection in a social dilemma setting in which individuals' effortful gains are unfairly distributed among group members. A stable "worker–parasite" relationship developed when three individually operant-conditioned rats were placed together in a Skinner box equipped with response lever and food dispenser on opposite sides. Specifically, one rat, the "worker," engaged in lever-pressing while the other two "parasitic" rats profited from the worker's effort by crowding the feeder in anticipation of food. Anatomically, c-Fos expression in the anterior cingulate cortex (ACC) was significantly higher in worker rats than in parasite rats. Functionally, ACC inactivation suppressed the worker's lever-press behavior drastically under social, but only mildly under individual, settings. Transcriptionally, $GABA_A$ receptor– and potassium channel–related messenger RNA expressions were reliably lower in the worker's, relative to parasite's, ACC. These findings indicate the requirement of ACC activation for the expression of exploitable, effortful behavior, which could be mediated by molecular pathways involving $GABA_A$ receptor/potassium channel proteins.

workload imbalance | labor exploitation | social dilemma | social decision-making | altruism

Exploitation of workload or labor in groups is a distinctive characteristic of social animals, ranging from worker ants (1) to humans (2). Social animals often have to decide how to behave in situations in which individuals' effortful gains are distributed unfairly in group dynamics. A canonical example of workload (or social distribution) inequities perhaps might be the Pareto principle, in which a minor subset (~20%) of an organization is generally responsible for the majority (~80%) of outcomes (3). Currently, the neurobiology underlying behavioral strategies of individuals' actions and gains in social settings involving workload imbalance is not well understood. Here, we examined the neural basis of the imbalance in workload distribution (or labor division) that naturally emerges using a task pioneered in 1940 by O.H. Mowrer (4), which he called a "social problem" task in rats. A "worker–parasite" relationship develops when rats individually trained in an operant conditioning chamber to press a lever on one wall and run to the opposite wall to consume dispensed food reward are placed together, typically in a cohort of three animals. This social situation initially causes all rats to stop pressing the lever, because the animal pressing the lever would be at a disadvantage to acquire food compared to those staying close to the feeder. This "stalemate" phase eventually transforms into a new behavioral equilibrium in which one rat ("worker") consistently (within- and between-sessions) performs nearly all lever presses, whereas the other rats ("parasites"), ignoring the lever, consume most of the reward. Subsequent studies have observed the worker–parasite separation among established workers (as well as parasites) (5, 6), using water as reward (6–9) and despite the availability of two levers and two reward dispensers (8, 10). When social hierarchy was examined as a driver of Mowrer's social problem (herein referred as worker–parasite problem/phenomenon), the relationship between hierarchy and worker–parasite behavior was complex. For example, submissive rats became workers when there was a high incidence of fighting (11), while dominant rats became workers when there was a low incidence of fighting (10). Selectively bred winners in a straight runway (tube) test had only a marginal propensity to become parasites (7). Despite extensive behavioral studies of the worker–parasite phenomenon, the mechanisms responsible for these individual differences have yet to be investigated.

Multiple neural systems have been implicated in various socially driven interactions and decision-making processes (12–15). The present study focused on the anterior cingulate cortex (ACC), because a large body of evidence from rodent, nonhuman primate, and human studies implicate ACC's roles in conflict monitoring (16), cost–benefit analysis for action selection (17, 18), and social cognition (15, 18–26), all of which can potentially be engaged in the worker–parasite problem. To do so, we compared the ACC activity with the emergence of worker's lever-press behavior and concomitant parasite's pellet-consuming behavior (4) and then examined the causal effects

NEUROSCIENCE

Significance

Although exploitation of labor in groups is a hallmark of social animals, its underlying neural mechanisms remain unknown. We explored this matter using a "social problem" paradigm in which one rat, the "worker," predominantly performed lever-pressing for food delivery while the other "parasitic" rats consumed nearly all delivered food by crowding the feeder in anticipation. We found that the anterior cingulate cortex (ACC) plays a necessary role in the worker's lever-press behavior under social situations, and that c-Fos immunoreactivity and $GABA_A$ receptor– and potassium channel–related messenger RNA expressions differed between the worker's and parasite's ACC. These results suggest that relative activation levels of the ACC could be a crucial factor determining the workload imbalance under social dilemma settings.

Author contributions: J.W.K., J.J.K., and M.W.J. designed research; S.A., Y.K., J.W.L., S.J.J., Y.J.L., S.L., J.K., and J.W.K. performed research; S.A., J.W.L., and S.J.J. analyzed data; and J.W.K., J.J.K., and M.W.J. wrote the paper.

The authors declare no competing interest.

This article is a PNAS Direct Submission.

Published under the PNAS license.

[1]S.A., Y.K., J.W.L., and S.J.J. contributed equally to this work.

[2]To whom correspondence may be addressed. Email: jawook.koo@kbri.re.kr, jeansokk@u.washington.edu, or mwjung@kaist.ac.kr.

This article contains supporting information online at http://www.pnas.org/lookup/suppl/doi:10.1073/pnas.2111145118/-/DCSupplemental.

Published November 23, 2021.

Downloaded at DGIST on November 26, 2021

of ACC inactivation on the worker's exploitable lever-press behavior. To test regional specificity, we also examined neural activity and inactivation effects of the amygdala, a structure implicated in emotional and value processing (27–32), social hierarchy (33, 34), and, more recently, social interaction and decision making (26).

It is unclear how the multifaceted ACC functions would influence the emergence of worker–parasite relationship in the social situations. Given that ACC lesions and inactivation decrease the choice of a high-reward/high-effort option over a low-reward/low-cost option in rats (35–38), the animal with relatively high ACC activity might become a worker because the prospect of reward, no matter how tenuous (high-effort/low-reward), is preferred than the no-reward option in prolonged stalemate phase (low-effort/no-reward). Alternatively, the worker–parasite separation might arise as an outcome of different subjective valuations of available behavioral options among rats. Given the putative role of the ACC in inferring intentions and motivations of others (15, 19–22), the ACC might play a role in assessing other rats' intentions to work or not, and this may determine the cost–benefit analysis for becoming a worker versus waiting for another rat to become a worker. Under this hypothesis, however, it is difficult to predict the ACC activity difference between worker and parasite animals. Another possibility is that aversion for disadvantageous inequity (39) might be a critical factor in worker–parasite separation. Previous studies have shown robust activation of the ACC when human subjects voluntarily reject an unfair offer during the ultimatum game (40). While it remains to be determined whether rats have a sense of fairness (41–43), we cannot exclude the possibility of unfair situation-induced ACC activity from preventing rats from pressing a lever. According to this view, the ACC activity would be higher in parasite than worker animals.

Here, we report that neural activity is higher in the worker's than the parasite's ACC and that inactivating the ACC suppresses the worker's lever-press behavior significantly under social, relative to nonsocial, settings. We further identified specific molecular changes in the worker's ACC that might elevate its neural activity. These findings provide insights into the neural mechanisms underlying workload imbalance that is universally observed in social animals.

Results

Worker–Parasite Separation in a Social Setting. Male Sprague–Dawley rats were trained individually to press a lever on one side of an enlarged Skinner box and retrieve a 20-mg food pellet on the opposite side (individual test; 90 min; Fig. 1*A* and Movie S1). When the performance reached a criterion of >100 presses/session for 3 consecutive d, separate groups of three animals were placed in the same box (group test; 90 min; Fig. 1*A*). In a group setting, animals quickly showed stalemate behavior (Movies S2 and S3) (i.e., they all crowded the feeder and seldom pressed the lever). After a period of impasse, which varied between groups (8.82 ± 1.27 d, n = 34 groups), a stable "worker–parasite" phase emerged across the days during which one rat ("worker") constantly began to press the lever at a high rate (>200 per session), while the other two ("parasite") rats continued to stay close to the feeder consuming most of the delivered pellets (Fig. 1 *B–D*, *SI Appendix*, Fig. S1, and Movies S4 and S5). Thus, there was no evidence of cooperation between animals taking turns at lever pressing and pellet consumption. Whether the animals became workers or parasites in this social task cannot fully be accounted by hunger motivation, motor activity, and anxiety factors, as their proxy variables (i.e., initial body weights [*SI Appendix*, Fig. S2] and propensity to lever press [*SI Appendix*, Fig. S3] during the individual test) were comparable between the groups. However, a subtle difference in the body condition contributing to the worker–parasite separation cannot be excluded. When the animal's mouth region was color marked to quantify food consumption, via a camera placed under a transparent feeder (n = 3 sessions from two groups), the workers attained only 8.2 ± 0.7% of all dispensed pellets.

Worker's Lever-Press Behavior Does Not Represent a Prosocial Behavior. To determine whether the workers' one-sided lever pressing represents a prosocial behavior, a subset of animals (n = 3 groups) were tested with a clear, perforated (1-cm diameter; 3.5 cm apart) partition in the box. Thus, the workers could press the lever, but they were unable to run to the feeder (Fig. 1*E*). With the partition, the workers' lever presses plummeted irrespective of the presence or absence of parasite animals at the feeder (one-way repeated-measures ANOVA, $F(2,4)$ = 223.010, $P = 7.9 \times 10^{-5}$; post hoc Sidak's test, group test versus group-divider test, $P = 1.9 \times 10^{-4}$; group test versus individual-divider test, $P = 1.4 \times 10^{-4}$; group-divider test versus individual-divider test, P = 0.526; Fig. 1*F*). This result indicates that the worker's lever-press behavior in the presence of other nonlever pressing (parasite) animals does not represent altruism.

Social Hierarchy between Worker and Parasite Rats. While there was active competition among the animals over the food (i.e., pushing each other from the feeder) during the group test, only sporadic incidents involved aggression, and there was no discernable evidence of dominance hierarchy (i.e., worker or parasite rats seldom displayed freezing and crouching defensive behaviors). To further assess whether the worker–parasite relationship is related to social hierarchy, following 3 d of worker–parasite relationship, we subjected the animals (n = 5 groups) to three different social dominance tests (Fig. 2*A*). In the "feeder" test (44), three rats competed for small (20 mg) food pellets delivered sporadically to the food cup according to a fixed-interval, 10-s schedule in the same Skinner box used for the worker–parasite problem task. In the "cylinder" test (4, 45), three rats competed for a large (5 g) food pellet in a small (diameter, 20 cm; height, 40 cm) cylinder. In the tube test (46, 47), two rats (three pairwise combinations of a worker and two parasites) competed to run through a tube (diameter, 6 cm; length, 80 cm) from the opposite sides to obtain a piece of cereal. The animal's behavior varied across sessions but stabilized over 3 to 21 d (*SI Appendix*, Fig. S4). In the feeder test, the worker collected the largest number of pellets (i.e., rank #1) in four groups, and the smallest number of pellets in one group (rank #3). In the cylinder test, the worker was in control of the food pellet for the longest duration (i.e., rank #1) in four groups and for the second longest duration (rank #2) in the other group. In the tube test, the worker was submissive to both parasites (i.e., rank #3) in all five groups (Fig. 2*B*). The likelihoods for five worker rats to be at the same rank by chance are 0.045 for three+ groups and 0.004 for all five groups (binomial test). These results indicate that the workers were generally dominant over the parasites in the feeder and cylinder tests but subordinate to the parasites in the tube test.

c-Fos Expression Is Higher in the Worker's ACC. We then examined the expression of c-Fos in the ACC of worker and parasite rats (n = 7 groups; a worker and a randomly chosen parasite from each group) following 3 consecutive d of worker–parasite separation (Fig. 3*A*). c-Fos expressions were also analyzed in the adjacent prelimbic cortex (PLC), implicated in social interactions (48–53), and the basolateral amygdala (BLA), implicated in emotional and value processing (27–32) and social decision making (26). The c-Fos-positive neurons were significantly elevated in workers than parasites in the ACC (t test, t (12) = 3.342, P = 0.006), but not in the PLC (t (12) = 0.568; P = 0.580) or BLA (t (12) = 1.205, P = 0.252; Fig. 3 *B* and *C*).

Downloaded at DGIST on November 26, 2021

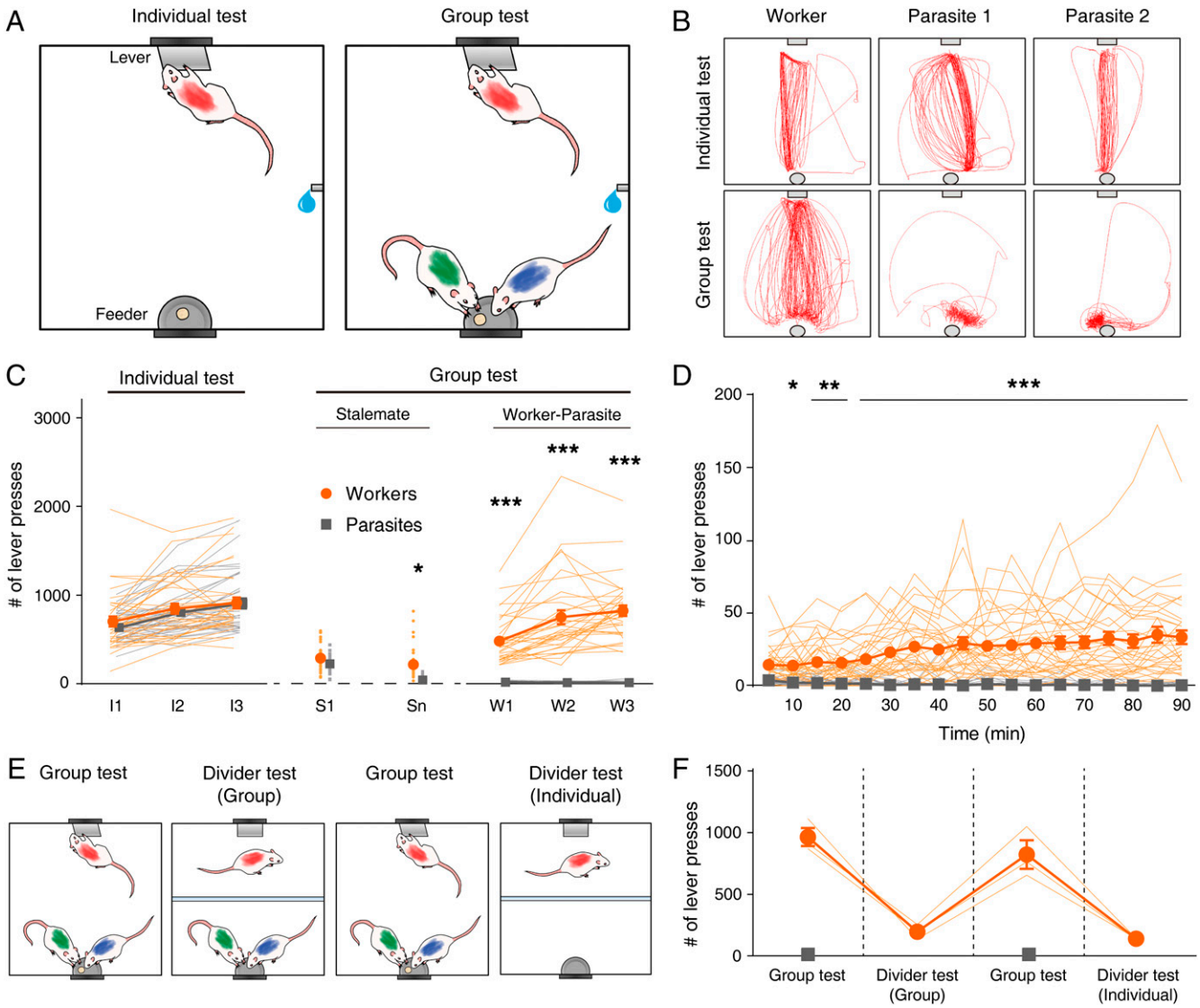

Fig. 1. Worker–parasite separation in a social setting. (*A*) Behavioral procedure schematics. Cohorts of three rats were trained individually to press a lever and retrieve a food pellet on the opposite side (individual test; 90 min) and then placed together (group test; 90 min). (*B*) Representative cumulative movement trajectories (5-min period) during individual test and group test sessions (sample I3 and W3 sessions, respectively, in *C*). (*C*) Lever-press behavior (n = 34 groups). I1–I3, individual test; S1 and Sn, the first and last days, respectively, of the "stalemate" phase of group test; W1 through W3, "worker–parasite" phase. (*D*) Time course of lever-press behavior during the first worker–parasite appearing session. (*E*) Experimental scheme for divider tests. A transparent barrier separated the chamber such that a worker rat could press the lever but not access the feeder. (*F*) Workers' lever-pressing behavior during divider tests. Orange, workers; gray, parasites. Thin, soft-colored lines and scattered small circles/squares, individual animal data; large circles/squares and error bars, group means and SEMs. *$P < 0.05$, **$P < 0.01$, and ***$P < 0.001$ (in *C* and *D*; workers versus parasites, post hoc Sidak's test following two-way repeated measures ANOVA). Parasite's lever-press frequency in this and subsequent figures represents averaged value obtained from two parasites of a group.

ACC Inactivation Suppresses the Worker's Lever-Pressing under Social Setting. Next, we tested the ACC's function in lever-pressing behavior during the worker–parasite problem task using cannulated animals (n = 6 groups). Following reliable worker–parasite separation (three consecutive sessions; W1 through W3), worker rats received muscimol bilaterally 30 min prior to group testing (Fig. 4*A*; histological identification of cannula locations in *SI Appendix*, Fig. S5). Intra-ACC muscimol infusions (session W4) caused the lever-press frequency of the workers to plummet to the level of parasites (two-way repeated measures ANOVA, sessions S1 to W5, main effect of animal type, $F(1,10) = 143.362$, $P = 3.0 \times 10^{-7}$; main effect of session, $F(6,60) = 13.850$, $P = 8.3 \times 10^{-10}$; animal type × session interaction, $F(6,60) = 19.073$, $P = 2.7 \times 10^{-12}$; post hoc Sidak's test, worker versus parasite on W3, $P = 2.2 \times 10^{-14}$; W4, $P = 0.997$; Movie S6). When retested without muscimol (session W5; artificial cerebrospinal fluid [ACSF] vehicle infusions in four rats and no infusions in two rats; data pooled because results were similar), the workers fully resumed their lever-pressing behavior (worker versus parasite on W5, $P < 1.0 \times 10^{-15}$; Movie S7 and Fig. 4 *B* and *C*).

The ACC inactivation effects were also examined in workers and parasites during individual tests on continuous reinforcement (CR) and partial reinforcement (PR) schedules. The PR rate was equated to the mean reinforcement rate of the worker rats (i.e., the number of pellets that workers consumed during the group test sessions [8%; see *Worker–Parasite Separation in a Social Setting*]). There were no reliable differences in movement speed,

NEUROSCIENCE

Downloaded at DGIST on November 26, 2021

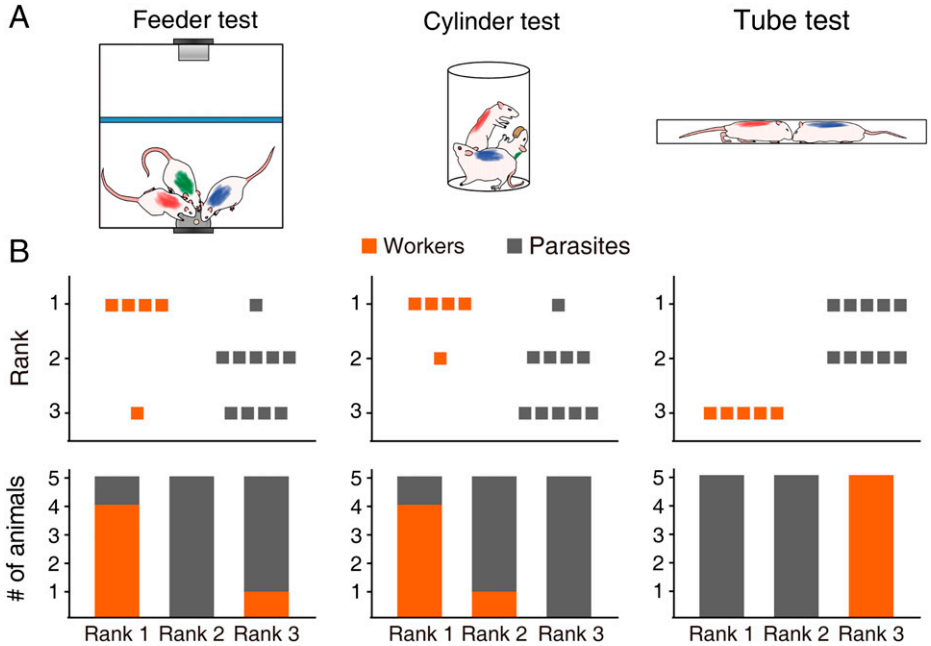

Fig. 2. Different social dominance between worker and parasite rats. (*A*) Schematics for the three social dominance tests used in the present study. (*Left*) Feeder test in the Skinner box. Small food pellets were delivered to the feeder in a fixed 10-s interval schedule, and the number of pellet consumption was compared across three rats. An opaque barrier (blue) blocked rat's access to the lever. (*Middle*) Cylinder test. A large food pellet was introduced to the center, and the duration of pellet possession was compared across three rats. (*Right*) Tube test. Two rats competed to run through a tube from the opposite sides to obtain a piece of cereal. (*B*) Group data showing the ranks of worker (orange) and parasite (gray) rats (n = 5 groups) during the stable behavioral phase. (*Top*) Individual animal data. (*Bottom*) Rank proportions of worker (orange) and parasite (gray) rats.

distance traveled, time spent in corners, and immobility duration between the group and PR schedule test settings (*SI Appendix*, Fig. S6), which suggests that worker rats exerted comparable levels of effort and anxiety across social and nonsocial settings. The controls for CR schedule comprised of ACSF and no infusions in four and two rats, respectively, and PR schedule included ACSF infusions in four rats. No significant effect of animal type was found in the lever-press frequency (two-way repeated measures ANOVA, CR schedule, sessions C1 to C3, main effect of animal type, $F(1,10) = 2.530$, $P = 0.143$; main effect of session, $F(2,20) = 11.879$, $P = 4.0 \times 10^{-4}$; animal type × session interaction, $F(2,20) = 0.320$, $P = 0.730$; PR schedule, sessions P1 to P2, main effect of animal type, $F(1,6) = 1.382$, $P = 0.284$; main effect of session, $F(1,6) = 1.202$, $P = 0.315$; animal type × session interaction, $F(1,6) = 0.216$, $P = 0.659$; Fig. 4 *B* and *C*). Further inspection across sessions indicated that muscimol also reliably decreased lever press during the individual test on CR schedule (post hoc Sidak's test, C1 versus C2, $P = 0.003$; C1 versus C3, $P = 0.895$; C2 versus C3, $P = 6.5 \times 10^{-4}$). However, the intra-ACC muscimol-induced suppression of the worker's lever-press frequency was significantly larger in the group test (W3 versus W4, 89.6 ± 3.6%) compared to the individual test on CR (24.4 ± 11.2%) and PR (16.0 ± 8.7%) schedules (one-way ANOVA, $F(2,13) = 23.022$; $P = 5.3 \times 10^{-5}$; post hoc Sidak's test, group test versus CR test, $P = 2.0 \times 10^{-4}$; group test versus PR test, $P = 1.8 \times 10^{-4}$; CR test versus PR test, $P = 0.888$; Fig. 4*D* and Movie S8). Hence, the ACC muscimol effects during the group test are not merely due to impaired motivation or motor functions. A similar conclusion was reached when we analyzed the frequency of lever-zone entry and the amount of time spent in the lever zone (*SI Appendix*, Fig. S7). Together, these results indicate that ACC plays an essential function in the worker's lever-press behavior under social settings.

Amygdala Inactivation Suppresses Lever-Pressing under both Social and Individual Settings. Although the amygdalae of workers and parasites showed no difference in c-Fos-positive neurons (Fig. 3*C*), given its putative roles in emotional and value processing (27–32), social hierarchy (33, 34), and social interaction/decision making (26), we examined the effect of amygdala inactivation on the rat's lever-press behavior (n = 5 groups; histological identification of cannula locations in *SI Appendix*, Fig. S5). A subset (n = 3 groups) of these rats were cannulated in both ACC and BLA bilaterally and tested in the order of ACC and then BLA inactivation (group and individual tests). Intra-BLA muscimol infusions (Fig. 5*A*) strongly suppressed the workers' lever-press behavior during the group test (Fig. 5 *B* and *C*). Unlike intra-ACC muscimol, however, intra-BLA muscimol powerfully suppressed lever-press behavior of the animals (both workers and parasites) during the individual test as well (Fig. 5 *B* and *C*). A two-way ANOVA was performed to examine the effects of brain regions (ACC versus BLA) and behavioral tests (group test versus CR test) on muscimol-induced changes in the lever-press frequency (percentage of suppression from the previous session). There was a significant interaction between the effects of brain regions and behavioral tests on muscimol-induced suppression of lever-pressing ($F(1,18) = 10.066$, $P = 0.005$). Simple main-effects analysis showed that the muscimol effect was stronger in the group test than individual test for ACC inactivation (Sidak's test, $P = 1.9 \times 10^{-4}$) but not for BLA inactivation ($P = 0.980$). Also, the muscimol effect was stronger for BLA than ACC inactivation in the individual test ($P = 8.4 \times 10^{-4}$), but not in the group test ($P = 0.999$; Fig. 5*D*). These results indicate that BLA inactivation suppressed lever-press behavior effectively during both group and individual tests, whereas ACC inactivation suppressed lever-press behavior preferentially during the group test. Hence, the BLA inactivation's general effect on lever-pressing is likely due to alterations in the motor (54) and/or motivation (55) functions.

Optogenetic ACC Inactivation Suppresses Worker's Lever-Pressing under Social Setting. To elaborate the muscimol findings, in another set of animals (n = 6 groups), we expressed inhibitory

Downloaded at DGIST on November 26, 2021

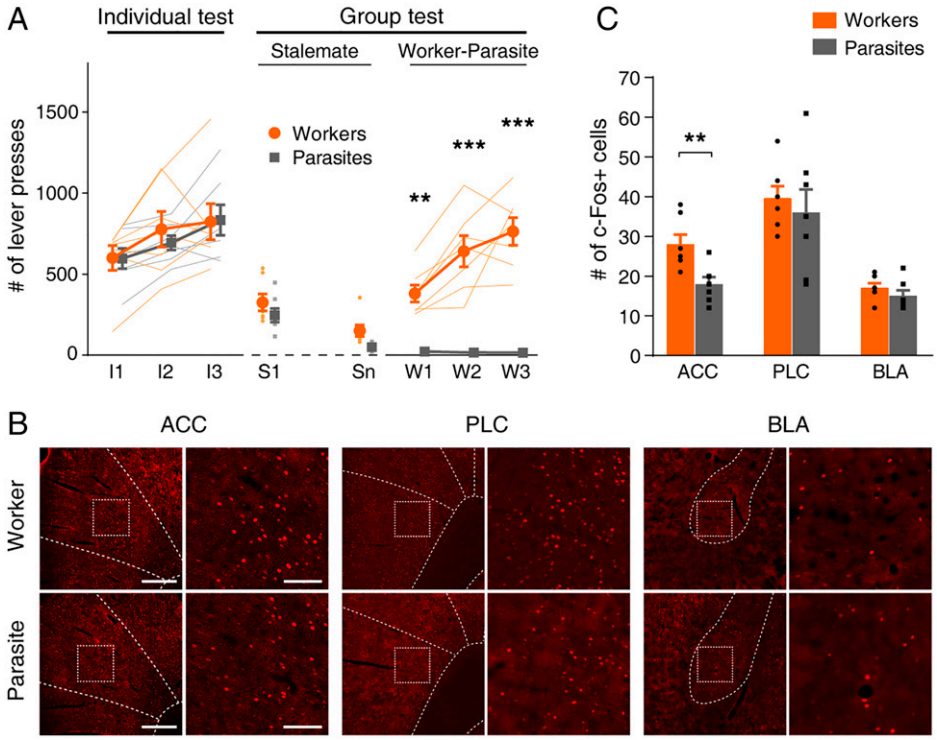

Fig. 3. c-Fos expression is higher in the worker's ACC. (*A*) Lever-press behavior of rats used in the c-Fos expression experiment ($n = 7$ groups). The duration of the stalemate phase varied between 3 and 8 d (4.86 ± 0.74; mean ± SEM). $^{**}P < 0.01$, $^{***}P < 0.001$ (workers versus parasites, post hoc Sidak's test following two-way repeated measures ANOVA). (*B*) Representative images of c-Fos immunoreactivity in coronal sections containing the ACC, PLC, and BLA. (Scale bar, *Left*, 400 μm; *Right*, 100 μm.) (*C*) Group data. $^{**}P < 0.01$ (workers versus parasites, *t* test). Thin, soft-colored lines and scattered small circles/squares, individual animal data; large circles/squares and bar graphs, group means; and error bars, SEMs.

opsin (eNpHR3.0) in ACC pyramidal neurons bilaterally (Fig. 6*A*). After worker–parasite separation for three consecutive sessions, the workers' ACC neurons were optically suppressed (histological identification of optical probe locations in *SI Appendix*, Fig. S5). To avoid optical bleaching, the duration of the group test was reduced to 30 min with alternating (and counter balanced) 5-min continuous-light stimulation and 5-min no-light stimulation periods (Fig. 6*B*). Though the optical inhibition effects were less pronounced than that of muscimol, the workers' lever-press frequency was significantly smaller during light-on periods compared to light-off periods (one-tailed paired *t* test, $t(5) = 2.483$, $P = 0.028$, $n = 6$ groups). By contrast, optical inhibition did not reliably decrease the lever-pressing behavior during the individual test on PR schedule ($t(5) = 1.226$, $P = 0.137$). In addition, the optical inhibition-induced, lever-press suppression (percentage of reduction compared with light-off periods) was significantly larger in group than individual testing (one-tailed paired *t* test, $t(10) = 1.876$, $P = 0.045$; Fig. 6 *C* and *D*). These results further suggest that ACC plays an important role in the workers' nonreinforced, lever-press behavior in a social context-dependent manner.

Differential Worker–Parasite Gene Expressions. Social behaviors and related psychiatric disorders have recently been associated with altered gene expressions in the ACC (25, 56). To capture these changes on a transcriptome-wide level, we performed RNA sequencing with ACC cells after the emergence of worker–parasite separation ($n = 4$ groups; *SI Appendix*, Fig. S8*A*). Sequencing data were subjected to principal component analysis (PCA). The PCA plot based on gene expression profiles showed distinct gene-wise clustering for worker versus parasite animals, which is primarily explained by principal component 2 (PC2, 9.57%; *SI Appendix*, Fig. S8*B*). This suggests that there are differentiated molecular mechanisms underlying the dichotomous behavioral phenotypes.

Differential expressed gene (DEG) analysis (fold change >1.3 and false discovery rate <0.05) (57, 58) identified 1,685 up-regulated and 1,224 down-regulated DEGs in the ACC from worker compared to parasite rats (Fig. 7 *A* and *B* and Dataset S1). Specifically, we observed large reductions of several potassium (K^+) channel subunit messenger RNAs (mRNA) in the ACC of workers in our DEGs list (*Kcna2*, *Kcnb2*, *Kcnc2*, *Kcnab3*, *Kcnh5*, and *Kcnip4*; Fig. 7*A*), which were corroborated by qRT-PCR performed on separate animal groups (two-way mixed ANOVA, main effect of gene, $F(5,54) = 1.177$, $P = 0.333$; main effect of animal group, $F(2,54) = 30.70$, $P = 1.1 \times 10^{-11}$; gene × animal group interaction, $F(10,54) = 0.509$, $P = 0.877$; Fisher's protected least square difference [PLSD] post hoc test, worker versus parasite, $P = 1.1 \times 10^{-11}$; worker versus home-cage control, $P = 1.1 \times 10^{-11}$; parasite versus home-cage control, $P = 0.439$; all $n = 4$ groups; post hoc test results for each gene are shown in Fig. 7*C*). We also observed distinctly lower expressions of several $GABA_A$ receptor subunits (*Gabra1*, *Gabrb1*, *Gabrb2*, and *Gabrb3*) and GABAergic transmission-related genes (*Gad2* and *Erbb4*) (59–61) in the ACC of workers (Fig. 7*A*), which were confirmed by qRT-PCR (main effect of gene, $F(5,54) = 0.957$, $P = 0.453$; main effect of animal group, $F(2,54) = 26.83$, $P = 1.1 \times 10^{-11}$; gene × animal group interaction, $F(10,54) = 0.354$, $P = 0.961$; worker versus parasite, $P = 1.1 \times 10^{-11}$; worker versus home-cage control, $P = 1.1 \times 10^{-11}$; parasite versus home-cage control, $P = 0.975$; all $n = 4$ groups; post hoc test results for each gene are shown in Fig. 7*D*). The down-regulation of the $GABA_A$ receptor subunits and their relevant genes together with the down-regulation of K^+ channel subunits are likely to contribute to the reduction of inhibitory tone and concomitant enhancement of excitatory tone in the

NEUROSCIENCE

Downloaded at DGIST on November 26, 2021

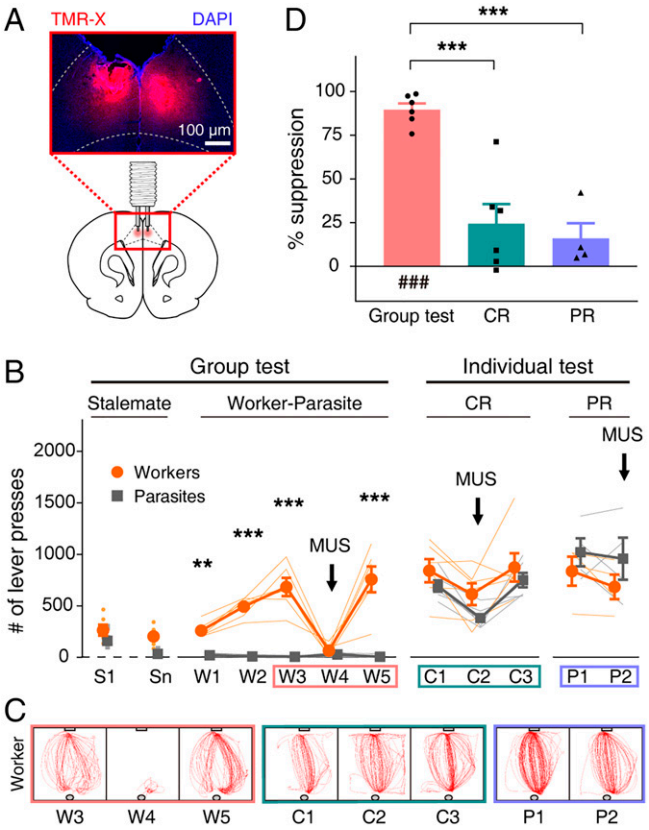

Fig. 4. ACC inactivation suppresses worker's lever-pressing under social setting. (*A*) Cannulae implant diagram and photomicrograph showing fluorescent muscimol (MUS) (TMR-X; red) spread in ACC. Blue, DAPI cell-body staining. (*B*) After the worker–parasite separation (sessions W1 through W3), workers were tested with (W4) and without (W5) MUS. Workers and parasites were then tested individually under CR (C1 through C3) and PR (P1 and P2) schedules with (C2 and P2) and without (C1, C3, and P1) MUS. $^{**}P < 0.01$, $^{***}P < 0.001$ (workers versus parasites, post hoc Sidak's test following two-way repeated measures ANOVA). (*C*) Representative movement trajectories (5-min period) of a worker +/− MUS during group and individual CR/PR tests. (*D*) MUS-induced suppression in lever presses (%) during group and individual CR/PR tests (compared to no-MUS conditions). $^{###}P < 0.001$ (difference from zero, one sample *t* test); $^{***}P < 0.001$ (difference between behavioral tests, post hoc Sidak's tests following one-way ANOVA). Thin, soft-colored lines and scattered small circles/squares, individual animal data; large circles/squares and bar graphs, group means; and error bars, SEMs.

ACC of worker animals. Such changes can explain the increased c-Fos-positive cell numbers (Fig. 3*C*) and increased expressions of the network disinhibition–induced (i.e., by treatment of bicuculline, a $GABA_A$ receptor antagonist, and 4-aminopyridine, a weak K^+ channel blocker), activity-responsive genes such as *Cyr61* and *Arc* (62, 63) but not of other activity-dependent genes such as *Adamts1* (64, 65) and *Slc2a1* (65, 66) in workers (Fig. 7*A*; qRT-PCR, main effect of gene, $F(4,73) = 2.151$, $P = 0.083$; main effect of animal group, $F(2,73) = 8.387$, $P = 0.001$; gene × animal group interaction, $F(8,73) = 1.700$, $P = 0.113$; worker versus parasite, $P = 0.002$; worker versus home-cage control, $P = 0.464$; parasite versus home-cage control, $P = 2.4 \times 10^{-4}$; all $n = 6$ groups; post hoc test results for each gene are shown in Fig. 7*E*).

Gene ontology (GO) enrichment analysis based on gene expression profiles revealed several notable terms about synaptic signaling (i.e., transsynaptic signaling, anterograde transsynaptic signaling, chemical synaptic transmission, ion transmembrane transport, etc.), particularly in down-regulated DEGs, in the ACC of the worker group (*SI Appendix*, Fig. S9 *A* and *B* and Dataset S2). Kyoto encyclopedia of genes and genomes (KEGG) pathway analysis of the down-regulated ACC DEGs identified certain GABAergic signaling-related pathways, including nicotine addiction and GABAergic synapse (*SI Appendix*, Fig. S9 *C* and *D* and Dataset S3) (67). A gene-coexpression network analysis also revealed significant gene–gene correlations among the GABAergic transmission-related genes (i.e., *Gabra1*, *Gabrb1*, *Gabrb2*, *Gabrb3*, and *Gad2*) and K^+ channel subunits (i.e., *Kcna2*, *Kcnc2*, and *Kcnab3*) in a subset of coexpression networks (*SI Appendix*, Fig. S9*E*). Overall, these results show down-regulation and up-regulation of network inhibitory and excitatory factors, respectively, in the ACC of the worker compared to parasite rats.

Discussion

Social animals often confront dilemma settings where individuals' effortful gains are unfairly distributed among group members. Here, we investigated the role of the ACC in action selection in a rodent model of Mowrer's social problem (4). Though a large number of studies in humans and monkeys implicated the ACC in social decision making, none has addressed the conundrum of workload imbalance, which is a shared behavioral characteristic in social animals (1, 2). The present study found that c-Fos expression (a marker for

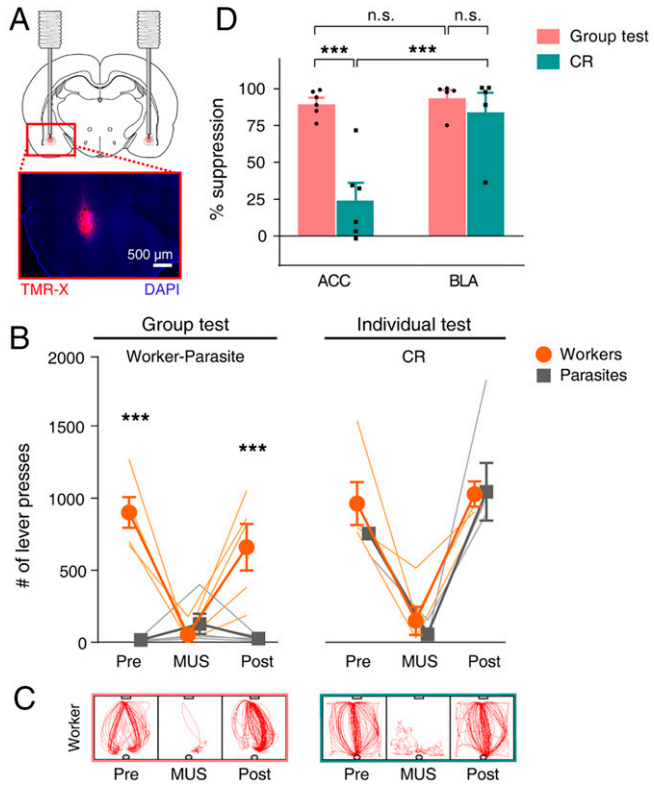

Fig. 5. Amygdala inactivation suppresses lever-pressing under both social and individual settings. (*A*) Cannulae implant diagram and photomicrograph showing fluorescent muscimol (TMR-X; red) spread in BLA. (*B*) Lever-press frequency with and without (Pre and Post) muscimol infusion into the BLA during the group (*Left*) and CR (*Right*) tests. $^{***}P < 0.001$ (between workers and parasites, two-way repeated measures ANOVA followed by post hoc Sidak's test). (*C*) Representative movement trajectories (5 min period) of a worker +/− muscimol during group and individual CR tests. (*D*) Comparison of ACC and BLA inactivation effects on lever-press frequency. Shown are normalized muscimol infusion effects (% suppression from the previous session). $^{***}P < 0.001$ (two-way ANOVA followed by post hoc Sidak's test). Thin, soft-colored lines and scattered small circles/squares, individual animal data; large circles/squares and bar graphs, group means; and error bars, SEMs.

Downloaded at DGIST on November 26, 2021

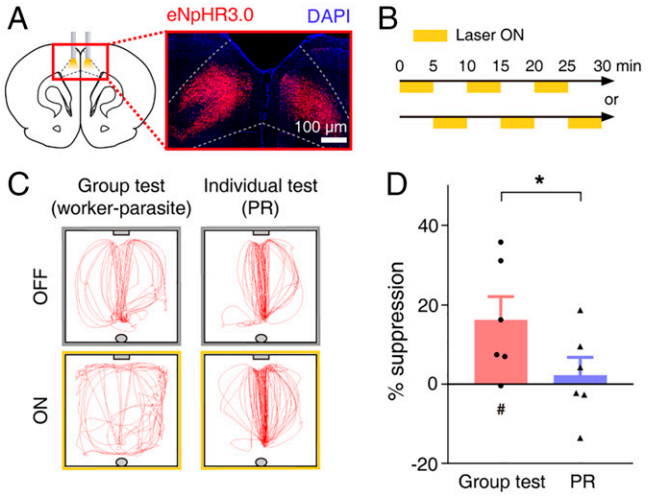

Fig. 6. Optogenetic ACC inactivation suppresses worker's lever-pressing under social setting. (*A*) A representative eNpHR3.0-mCherry expression in ACC. (*B*) Alternating 5 min light on/off stimulations for 30 min. (*C*) A worker's movement trajectories (5 min) during group and individual tests with (ON) or without (OFF) light-stimulation. (*D*) Light-induced lever-press suppression (% reduction from no-stimulation). $^{\#}P < 0.05$ (difference from zero, one sample *t* test); $^{*}P < 0.05$ (difference between behavioral tests, one-tailed paired *t* test). Scattered small circles/triangles, individual animal data; bar graphs, group means; and error bars, SEMs.

neuronal activity) was significantly higher in the worker's than parasite's ACC. The increased c-Fos reactivity in ACC appears to be localized, as neither PLC, an adjacent structure implicated in social interactions (36–41), nor BLA, implicated in emotional and value processing (42–46), revealed a reliable increase. We then showed that pharmacological and optogenetic inactivation of the ACC reliably suppressed the worker's lever-press behavior. Importantly, the fact that the same manipulations only weakly suppressed lever presses in worker rats during individual (nonsocial) tests, under both continuous-reinforcement and partial-reinforcement schedules, suggests that the ACC plays an essential function in the worker's socially driven lever-press behavior. Contrary to the ACC, the BLA inactivation suppressed the worker's lever-press behavior strongly under both social and nonsocial contexts. Hence, the generalized effects of BLA inactivation could be due to impairing the hunger motivation and/or the sensory–motor function. Together, these results indicate that the relative activation level of the ACC is a crucial determinant for the behavioral strategies in a social dilemma setting with workload imbalance. Our study further suggests a putative molecular mechanism underlying the expression of the worker's exploitable effortful behavior. The DEG analysis from RNA-sequencing data revealed reduced expressions of GABA signaling-related proteins and K^+ channels in the ACC of worker animals. These changes may contribute to decreasing local inhibitory tone in the ACC neural network. Previous in vitro studies have shown that burst firing of excitatory neurons is enhanced by bicuculline, which augments excitatory synaptic potentials, and 4-aminopyridine, which prolongs action potential duration (64). A gene-profiling study using this commonly used protocol for neuronal stimulation found elevation of some unique genes such as *Cyr61* and *Arc* (63). We also observed higher levels of these network disinhibition–responsive factors in the ACC of workers compared with parasites. Together, these results suggest that the excitatory activity of the worker's ACC is elevated by reduced GABA- and K^+ channel-related proteins (i.e., via network disinhibition), which in turn promotes effortful behavior in a social dilemma setting (*SI Appendix*, Fig. S10). Accordingly, the absence of a worker–parasite relationship in a small fraction of groups ($n = 6$ out of 40, 15%, with extended 18 testing sessions) may be due to none of the animals having these molecular changes in their ACC sufficiently above the threshold for initiating the lever-press behavior.

A pertinent issue is whether appropriate patterns of ACC excitation can promote the lever-pressing behavior in parasite animals under a social dilemma setting. In a similar vein, it would be interesting to examine whether the excitation of ACC during the stalemate phase causes the stimulated animal to promptly become a worker. We were unable to test these possibilities in the present study, because ACC activation, via $GABA_A$ receptor antagonist (bicuculline) or optogenetics, produced seizures in the animals. Thus, other methods of stimulating the ACC in a physiological range is needed to determine whether enhancing the ACC neural activity can transform parasitic (exploiting) behavior into worker-like (exploitable) behavior.

Functionally, it would be advantageous for individuals to exploit other's labor to maximize their food intake while conserving energy expenditure. This is presumably reflected in all rats' tendencies not to press the lever during the stalemate phase. On the other hand, the threshold for emitting an exploitable behavior (i.e., the lever press), if too high, could potentially be self detrimental. Therefore, the threshold to initiate an exploitable behavior, which is likely to vary widely depending on behavioral settings, might be an outcome of these two opposing evolutionary pressures (i.e., the beneficial consequence to self from successfully exploiting others versus the detrimental consequence to self from unsuccessfully exploiting others). One of its outcomes that affects individuals in group dynamics might be the previously mentioned Pareto principle universally observed in social animals (3).

The ACC has been implicated in the cost–benefit analysis for action selection and social decision making (15, 17, 18, 20, 21, 26, 68). The results from our study show that the ACC is necessary for the expression of the worker's exploitable lever-press behavior (resulting in a very low probability of reward) under a social dilemma setting. However, it is unclear how the social cognition and cost–benefit analysis functions proposed for the ACC precisely contribute to the worker–parasite separation. Our results are consistent with the possibility that the ACC performs a cost–benefit analysis incorporating social factors in the process of selecting effortful reward-seeking behavior. Specifically, the ACC might serve as the center of the brain where the information on social competition is integrated with cost–benefit for different behavioral options (69). The outcome of such integration might determine the bias toward selecting an effortful but more-rewarding behavioral option. Note, however, that a worker–parasite separation may be achieved via multiple processes, and the present study does not provide unambiguous evidence for a particular mechanism. Clearly, further studies are needed to understand how the ACC integrates social and nonsocial information in guiding choice behavior and how such ACC functions manifest in different types of social dilemma settings.

Whether the present study's worker–parasite relationship is directly related to social hierarchy is unclear based on the results of three standard social dominance tests. We found significant relationships between the animals' lever-press behavior and subsequent social ranks, which suggests that whether a rat becomes a worker or a parasite may be related to social hierarchy. However, while significant positive relationships were found between the rats' lever-press behavior and their subsequent social ranks in feeder and cylinder tests, a negative relationship was observed with the tube test. As inconsistent patterns of social hierarchy across different social dominance tests in rats are not uncommon (7, 70–72), the factor(s) crucial for winning competition

Downloaded at DGIST on November 26, 2021

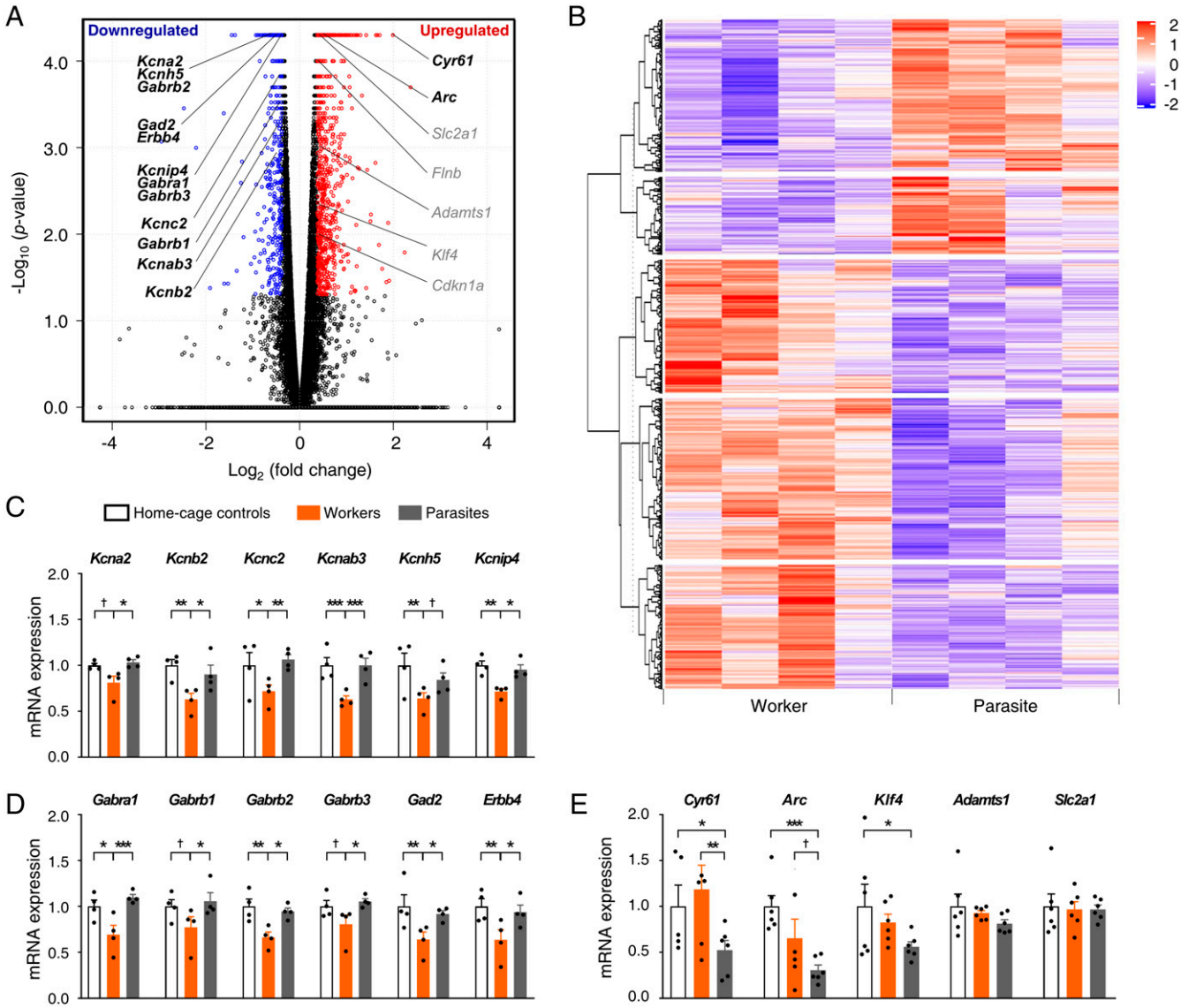

Fig. 7. Differential worker–parasite gene expressions. (*A*) Volcano plot highlighting DEGs ($n = 4$ groups). (*B*) Heatmap illustration of DEGs with a red-to-purple gradient depicting up-regulation (red) and down-regulation (purple). (*C–E*) Validation of RNA-sequencing results by qRT-PCR (mean ± SEM; $n = 4$ groups in *C* and *D*; $n = 6$ groups in *E*). (*C*) mRNA expression levels of some K^+ channel subunits were reduced in workers' compared to parasites' ACC. (*D*) Specific $GABA_A$ receptor subunit and GABA signaling–related gene expressions decreased in workers' ACC. (*E*) In contrast, a subset of activity-responsive genes was higher in workers' than parasites' ACC. $^{\dagger}P < 0.1$, $^{*}P < 0.05$, $^{**}P < 0.01$, and $^{***}P < 0.001$ (Fisher's PLSD test following two-way mixed ANOVA) (88, 90). Refer also to Dataset S1 and *SI Appendix*, Table S1 and Figs. S8–S10.

might vary depending on the exact structure of a dominance test (34). Previous behavioral studies (5, 6, 9) examined a priori relationship between the animals' social ranks and their lever-press behavior in the worker–parasite task and found that more active rats tended to become workers and aggressive, because they get less rewards. With respect to dominance hierarchy, aggression was suggested to be a byproduct rather than a causal factor of the worker–parasite relationship (8), which is consistent with our feeder and cylinder test results. It appears then the present worker–parasite (behavioral, anatomical, functional, and molecular) results cannot be explained by a simple, unified social dominance hierarchy.

There remain other outstanding issues to be investigated regarding the relative activation levels of the ACC and the workload imbalance under social dilemma setting, such as whether the molecular changes observed in the worker's ACC (reduced expressions of network inhibitory factors—GABA-related proteins and K^+ channels) are sufficient for the expression of lever-press behavior. This can be examined in future studies using small interfering RNA and related technologies. Also, to be further determined are factors that initiate down-regulation of GABA-related proteins and K^+ channels, downstream neural circuits mediating ACC neural activity to behavioral responses, and neural coding of the worker's effortful behavior under social dilemmas.

Materials and Methods

Subjects. A total of 127 young-adult male Sprague–Dawley rats (~8 to 10 wk old, 275 to 325 g) were used. They were individually housed in a climate-controlled colony room. After 1 wk of free access to food and water and habituation to handling, animals were placed on standard food restriction to gradually reach and maintain 80 to 85% normal weight. Of the total, 117 rats were trained for worker–parasite relationship (40 groups; three rats were used in two different groups of worker–parasites), and 10 rats were used as

Downloaded at DGIST on November 26, 2021

home-cage controls. Out of 40 groups tested, six failed to show worker–parasite relationship even with prolonged testing (18 d of stalemate) and thus were excluded from the analysis. All tests were performed during the dark phase of a 12-h light/dark cycle, and all animal care and experimental procedures complied with protocols approved by the directives of the Animal Care and Use Committee of Korea Advanced Institute of Science and Technology (approval number KA2018-08).

Apparatus. Four customized Skinner boxes (60 × 60 × 60 cm; Noldus PhenoTyper chambers) were used, each equipped with a lever (4.5 × 2 cm) on the North wall, a feeder (made of stainless steel or transparent acrylic; 3-cm diameter), and a light-emitting diode (LED) light (8 cm above the feeder) on the South wall, and a waterspout on the East wall (Fig. 1*A*). A lever press turned on the LED light (for 1 s) and delivered a food pellet (20 mg, Bio-Serv). An overhead camera (Basler; 120 cm above the floor) and Ethovision XT system (Noldus) were used to track the movements of three animals (marked Red, Green, or Blue on their back) simultaneously. In one of the chambers, a movie camera (Supereyes) was placed under the transparent acrylic feeder to record pellet-retrieval activities of rats.

Worker–Parasite Problem Task. Animals underwent successive 90-min sessions of habituation (2 d of chamber familiarization) and shaping-CR schedule training (variable days to reach 100 lever presses/session for 3+ days) prior to group testing (Fig. 1*C*). On the first day of group testing, the lever-pressing behavior rapidly plummeted in all rats (stalemate phase). The length of stalemate days varied between groups before a worker–parasite relationship emerged in which one rat performed most of the lever presses, while the other two members consumed most of the food pellets. The criterion for worker–parasite phase was defined as >200 lever presses by the worker rat, exceeding two parasites' lever presses by >150 for 3+ consecutive sessions. A total of 34 groups of three rats met the worker–parasite separation criterion. Six groups that failed to show clear worker–parasite separation after 18 d were excluded from the analysis. Following the group test, 16 groups were further tested in the CR and/or PR (8% probability of food, matching the worker's food consumption rate during group testing) schedule individual tests. Of the 34 groups that formed worker–parasite relationship, three groups were used for the divider test, seven groups for examining c-Fos expressions, six groups for ACC inactivation with muscimol, five groups for BLA inactivation with muscimol (three groups were used for both ACC and BLA inactivation), six groups for optogenetic inactivation of ACC, five groups for examining social hierarchy (of which two groups were used for both BLA inactivation and social hierarchy), four groups for RNA sequencing, and six groups for qRT-PCR. In optogenetic experiments, the session was shortened to 30 min to avert optical bleaching.

Social Hierarchy Tests. Five groups of rats were subjected to three different social hierarchy tests following three stable days of worker–parasite relationship. A subset of the rats ($n = 2$ groups) had a prior experience of amygdala inactivation; following the completion of the amygdala inactivation test (Fig. 5), a stable work–parasite relationship was confirmed for three sessions before being tested for social hierarchy. In the feeder test (44), three rats competed for food pellets in the same Skinner box used in the main worker–parasite problem experiment, except that an opaque barrier was placed 27 cm away from the north wall blocking rats' access to the lever, and a 20-mg food pellet was delivered to the food cup on a fixed interval (10 s) schedule. The number of food pellets retrieved by each rat during a 10-min session was used as the index for social hierarchy. In the cylinder test (4, 45), three rats competed for a large (5 g) food pellet in a small (diameter, 20 cm; height, 40 cm) transparent cylinder until the food pellet was consumed or for 10 min, following one individual habituation session in the cylinder in the previous day during which they were allowed to consume a 5-g food pellet. The total duration of clutching the food pellet was used as the index for social hierarchy. In the tube test (46, 47), two rats competed to run through a transparent tube (diameter, 6 cm; length, 80 cm) from the opposite sides to obtain a piece of Oreo O's cereal (Post Consumer Brands). Each rat was trained individually to run through the tube five times from each end (total 10 trials) to obtain a piece of Oreo O's cereal for 2 d before being tested in the tube test. All three pairwise combinations of three rats (a worker and two parasites) were tested in each day, and the rank was determined by the number of wins. In the feeder and cylinder tests, each group was tested until the same animal was at the top rank for three consecutive days (stable phase; *SI Appendix*, Fig. S4). The rat's social rank was determined based on the mean number of small food pellets consumed (feeder test) or the mean possession time of a large food pellet (cylinder test) during the stable phase. In the tube test, each group was tested until all of its members maintained the same ranks for 4 consecutive d (stable phase; *SI Appendix*, Fig. S4). The rats' social ranks during the stable phase were determined to be their social ranks in the tube test. Four groups of rats performed the tests in the order of the feeder, cylinder, and tube tests, and one group was tested in the order of the cylinder, tube, and feeder tests. The observed ranks could not be explained by the order of the tests, indicating that the test order did not affect social hierarchy.

c-Fos Staining and Counting. A total 1 h after the emergence of worker–parasite relationship, a subset of rats ($n = 14$; a worker and a randomly chosen parasite from each of $n = 7$ groups) was used for c-Fos staining. Animals were perfused intracardially with phosphate-buffered saline (PBS, pH 7.4) followed by 4% paraformaldehyde (PFA) fixative. The brains were removed, postfixed overnight in 4% PFA, and subsequently immersed in 30% sucrose in PBS solution at 4 °C. Coronal sections (40 μm) of the brain were prepared according to a standard histological procedure (73). For immunohistochemistry, brain sections containing medial prefrontal cortex (ACC and PLC) and amygdala (BLA) were washed with PBS for 3 × 10 min and incubated in blocking solution (0.3% trinton-X100 and 4% normal donkey serum in PBS) for 1 h at room temperature. Tissues were incubated with the primary antibody rabbit anti-c-Fos (#ABE457, 1:1,000, Merck Millipore) overnight at 4 °C. Following 3 × 10 min washing in PBS, incubation with the secondary antibody (Alexa555 donkey anti-rabbit, #A-31572, 1:500, Thermo Fisher Scientific) was done for 3 h at room temperature. All tissues were rinsed with PBS for 3 × 10 min, mounted on slides (Muto pure chemicals), and cover-slipped with Vecta-Mount mounting medium (Vector Laboratories). Imaging and cell counting were done using the equipment of the Brain Research Core Facilities at Korea Brain Research Institute. All images were obtained with a Pannoramic Scan (3DHistech) at equal gain and exposure with a 20× objective and then converted to the tagged image file format using ImageJ. For analysis of cell counts, the spot function in Imaris software (Bitplane) was used. The number of c-Fos-positive cells was automatically calculated under the same intensity threshold in each image. The region of interest (400 × 400 μm) and analysis of cell counts were determined by a blind observer.

Pharmacological Inhibition. Animals ($n = 6$ groups) underwent a standard cannula implantation surgery before behavioral training. Under isoflurane (1.5 to 2.0% [vol/vol] in 100% oxygen) anesthesia, small burr holes (4 mm diameter) were drilled on the skull, and a dual 26-gauge guide cannula was implanted into ACC (from bregma: +2.6 mm anterior, 0.6 mm lateral, and −1.6 mm and ventral). Three groups of rats further received cannulae implants in their BLA (from bregma: −2.3 mm posterior, 5 mm lateral, 7.8 mm ventral). Two additional groups of rats received cannulae implants only in their BLA. On the drug test day, muscimol (Sigma-Aldrich) dissolved in ACSF was infused into ACC or BLA (10 mM, 0.3 μL per side, and 0.1 μL/min) via 33-gauge infusion cannulae that protruded 1 mm beyond the guide cannulae using a 10-μl Hamilton microsyringe driven by a LEGATO 200 microsyringe pump (KD Scientific Inc.). The injection needle was held in place for 3 min postinjection. Behavioral testing started 30 min after muscimol or ACSF infusion into the ACC but 4 h after muscimol/ACSF infusion into the BLA to minimize motor-impairment effects (54).

Optogenetic Inhibition. Under isoflurane anesthesia, small burr holes were drilled on the skull bilaterally (from bregma: +2.6 mm anterior and 1.18 mm lateral), and 1 μL of virus carrying halorhodopsin (AAV9-CaMKIIα-eNpHR3.0-mCherry, The Vector Core at the University of North Carolina at Chapel Hill) was injected 2.3 mm below the skull surface with a 10° angle toward the midline targeting the ACC bilaterally at a rate of 0.05 μL/min. The injection needle was held in place for 10 min postinjection. Then, optical fibers (200 μm diameter) were implanted bilaterally in the ACC (1.8 mm below the skull surface). Optical stimulation experiments were performed 4 to 7 wk following the surgery. For optogenetic inactivation of ACC neurons, a continuous 594-nm laser stimulation (5 to 15 mW; Changchun New Industries Optoelectronics Tech.) was delivered for 5 min, alternating with 5 min of no stimulation for 30 min (a total of 15 min stimulation). Optogenetic inactivation was repeated over two daily sessions with the order of stimulation–no stimulation sequence counterbalanced.

Histology. The extent of eNpHR3.0 expressions, cannula tracks, and optic fiber tracks were verified by examining coronal section (40 to 50 μm) brain images obtained (10×) with a Zeiss Axio Scan.Z1 slide scanner (Zeiss) following a standard histological procedure (74) with Nissl and/or DAPI staining. The extent of muscimol diffusion in ACC was examined using fluorescent muscimol (Bodipy TMR-X) in two rats (75).

RNA Sequencing. Animals (a worker and a randomly chosen parasite from each of four animal groups) were rapidly decapitated 18 to 19 h after the

NEUROSCIENCE

Downloaded at DGIST on November 26, 2021

worker–parasite relationship transpired in group testing. An additional four animals not exposed to the Skinner box were euthanized as home-cage controls. Brains were removed, and coronal slices (2 mm) were dissected in a cold brain matrix. ACC were then microdissected, as depicted in *SI Appendix*, Fig. S8*A*, using a dissecting microscope and reference coordinates obtained from the Paxinos and Watson rat brain atlas (76). RNA was isolated with TriZol reagent (Invitrogen) and purified with RNeasy Mini Kits (Qiagen). All RNA samples were determined to have RNA integrity number values > 8.5 (4200 Tapestation) for RNA sequencing. Library preparations and sequencing were performed by Theragen Bio Inc. (Suwon, South Korea). A total 200 ng of purified RNA was used to prepare libraries for sequencing using the TruSeq Stranded mRNA Sample Prep kit (Illumina). Libraries were sequenced on an Illumina NovaSeq platform to generate 100-bp paired-end reads. Sequencing data are deposited at Gene Expression Omnibus (GEO) and available through accession number GSE153649 (https://www.ncbi.nlm.nih.gov/geo/query/acc.cgi?acc=GSE153649).

Differential Expression Analysis. After the acquisition of read sequences for each sample, we assessed the quality of raw reads in fastq format (77). Once the sequence of the reads was determined, they were aligned to the reference genome (Rnor_6.0/Ensembl 77) using TopHat software (78). We then used the Cufflinks version 2.1.1 to construct and identify both known and novel transcripts from the TopHat alignment results (79). Expression profile was extracted from Fragments Per Kilobase of transcript per Million mapped reads value by expression quantification obtained from the transcript quantification of each sample. We used the Cuffdiff to identify DEGs (80), and the adjusted *P* values were corrected by the Benjamini–Hochberg method for controlling the false discovery rate (81). Genes with a fold change ≥1.3 and *P* value < 0.05 were considered as differentially expressed.

Enrichment, Pathway, and Network Analysis. To identify cellular processes represented by the DEGs, we carried out a functional enrichment analysis of GO biological processes (GOBPs) using the Database for Annotation, Visualization and Integrated Discovery (DAVID) functional annotation tool (version 6.8) (82). The GOBPs represented by a list of the DEGs were identified as genes with modified Fisher's exact *P* values < 0.05 (Fisher, 1922) and a gene count ≥3 (83). KEGG pathway annotation was also performed using the DAVID gene annotation tool (https://david.ncifcrf.gov/). To reveal functional interactions among the DEGs, the Search Tool for the Retrieval of Interacting Genes/Proteins database (version 11) was explored for the protein–protein interactions (PPI) (84). PPIs with confidence score <0.4 (a commonly used threshold) was discarded and disconnected nodes were hidden. The resulting interaction network was imported into Cytoscape version 3.6.0 (85) for visualization. Clusters in the interaction data were identified using the Cytoscape plug-in clusterMaker version 2 (86). We used "community clustering (GLay)" with the default options, which provides an optimized layout for large networks and a structured visualization for more efficient exploration and analysis of biological networks (87).

RNA Extraction and qRT-PCR. Animals (total six groups; the parasites' mRNA expression levels were averaged for each animal group) were rapidly decapitated (unanesthetized) 18 to 19 h after the emergence of worker–parasite relationship. An additional six animals unexposed to the Skinner box were euthanized as home-cage controls. Brains were removed, frozen in dry ice, and stored at −80 °C to be dissected afterward. Coronal slices (1 mm) were dissected in a cold brain matrix from the previously frozen brains and ACC were microdissected, as depicted in *SI Appendix*, Fig. S8*A*. For RNA isolation, the microdissected ACC tissue samples were processed according to a published protocol (88). RNA was reverse transcribed into complementary DNA (cDNA) using an iScript cDNA synthesis kit (BioRad). Primers were designed to amplify regions of 100 to 250 bp located within the target genes (*SI Appendix*, Table S1). SYBR Green qRT-PCR was run in triplicate on the LightCycler480 Instrument II (Roche) and analyzed using the ΔΔCt method as previously described (89) with glyceraldehyde-3-phosphate dehydrogenase (*Gapdh*) as a normalization control.

Statistical Tests. Results are presented as mean ± SEM unless noted otherwise. To match the sample size of workers, the data collected from two parasites in each group were averaged and the outcome was treated as one data point unless otherwise stated. All statistical analyses were performed with Prism (version 8.2.1; GraphPad Software). Two-way ANOVA was performed to compare lever-press behavior of the animals (group factors: animal groups and test sessions or brain areas and behavioral tests) and the mRNA expression levels (group factors: animal groups and genes). One-way ANOVA was performed to compare lever-press behavior with and without a divider in the Skinner box and to compare muscimol effects on lever-press behavior during the group, CR, and PR tests. A binomial test was used to determine whether the distribution of worker's social ranks is significantly different from that expected by chance. All other comparisons were performed with Student's *t* tests. All statistical tests were two-tailed unless noted otherwise.

Data Availability. Sequencing data are available at Gene Expression Omnibus (accession number: GSE153649; https://www.ncbi.nlm.nih.gov/geo/query/acc.cgi?acc=GSE153649). Other datasets that support the findings of this study are available at Mendeley Data (accession code: https://dx.doi.org/10.17632/jt2nntv7b3.1).

ACKNOWLEDGMENTS. We thank Lynn Nadel and Richard Palmiter for their helpful comments on the earlier version of the manuscript and Hackjin Kim for helpful discussion on ACC's role in social cognition. We also thank B.S. Kang (SYSOFT) for analyzing the RNA-sequencing data and the Korea Brain Research Institute Brain Research Core Facilities for technical assistance in the image processing. This work was supported by the Research Center Program of Institute for Basic Science (IBS-R002-A1; M.W.J.), NIH (MH099073 and AG067008; J.J.K.), the National Research Foundation of Korea (2017M3C7A1048089; J.W.K.), and the Korea Brain Research Institute basic research program (20-BR-04-03; J.W.K.)

1. D. Charbonneau, T. Sasaki, A. Dornhaus, Who needs 'lazy' workers? Inactive workers act as a 'reserve' labor force replacing active workers, but inactive workers are not replaced when they are removed. *PLoS One* **12**, e0184074 (2017).
2. K. Marx, *Capital: A Critique of Political Economy* (C.H. Kerr & Company, Chicago, 1906).
3. L. Kaplow, S. Shavell, Any non-welfarist method of policy assessment violates the Pareto principle. *J. Polit. Econ.* **109**, 281–286 (2001).
4. O. H. Mowrer, Animal studies in the genesis of personality. *Trans. N. Y. Acad. Sci.* **3**, 8–11 (1940).
5. H. Oldfield-Box, Social organization of rats in a "social problem" situation. *Nature* **213**, 533–534 (1967).
6. J. Masur, V. Aparecidadasilva, Fighting behavior displayed during development of a worker-parasite relationship between rats. *Behav. Biol.* **20**, 51–59 (1977).
7. T. Fukasawa, M. P. Lima, J. Masur, The behavior of genetically selected loser and winner-runway rats in different competitive situations. *Behav. Biol.* **15**, 333–342 (1975).
8. J. Masur, V. Aparecida da Silva, M. T. Leonardi Radicchi, An attempt to prevent the development of a worker–Parasite relationship between rats. *Behav. Biol.* **19**, 380–388 (1977).
9. Y. Kataoka, K. Shibata, M. Fujiwara, S. Ueki, Basic studies on labor division between rats–A re-evaluation. *Behav. Neural Biol.* **34**, 89–97 (1982).
10. G. T. Taylor, Agonistic behavior and maintenance of a learned response in male rats. *Behav. Biol.* **19**, 491–502 (1977).
11. G. T. Taylor, S. Moore, Social position and competition in laboratory rats. *J. Comp. Physiol. Psychol.* **88**, 424–430 (1975).
12. D. Lee, Game theory and neural basis of social decision making. *Nat. Neurosci.* **11**, 404–409 (2008).
13. J. K. Rilling, A. G. Sanfey, The neuroscience of social decision-making. *Annu. Rev. Psychol.* **62**, 23–48 (2011).
14. C. C. Ruff, E. Fehr, The neurobiology of rewards and values in social decision making. *Nat. Rev. Neurosci.* **15**, 549–562 (2014).
15. S. Tremblay, K. M. Sharika, M. L. Platt, Social decision-making and the brain: A comparative perspective. *Trends Cogn. Sci.* **21**, 265–276 (2017).
16. M. M. Botvinick, J. D. Cohen, C. S. Carter, Conflict monitoring and anterior cingulate cortex: An update. *Trends Cogn. Sci.* **8**, 539–546 (2004).
17. S. W. Kennerley, M. E. Walton, Decision making and reward in frontal cortex: Complementary evidence from neurophysiological and neuropsychological studies. *Behav. Neurosci.* **125**, 297–317 (2011).
18. M. F. Rushworth, T. E. Behrens, P. H. Rudebeck, M. E. Walton, Contrasting roles for cingulate and orbitofrontal cortex in decisions and social behaviour. *Trends Cogn. Sci.* **11**, 168–176 (2007).
19. D. M. Amodio, C. D. Frith, Meeting of minds: The medial frontal cortex and social cognition. *Nat. Rev. Neurosci.* **7**, 268–277 (2006).
20. M. A. Apps, M. F. Rushworth, S. W. Chang, The anterior cingulate gyrus and social cognition: Tracking the motivation of others. *Neuron* **90**, 692–707 (2016).
21. T. E. Behrens, L. T. Hunt, M. F. Rushworth, The computation of social behavior. *Science* **324**, 1160–1164 (2009).
22. M. K. Wittmann, P. L. Lockwood, M. F. S. Rushworth, Neural mechanisms of social cognition in primates. *Annu. Rev. Neurosci.* **41**, 99–118 (2018).
23. K. Haroush, Z. M. Williams, Neuronal prediction of opponent's behavior during cooperative social interchange in primates. *Cell* **160**, 1233–1245 (2015).
24. M. Carrillo, Y. Han, F. Migliorati, M. Liu, V. Gazzola, C. Keysers, Emotional mirror neurons in the rat's anterior cingulate cortex. *Curr. Biol.* **29**, 1301–1312.e6 (2019).
25. B. Guo *et al.*, Anterior cingulate cortex dysfunction underlies social deficits in Shank3 mutant mice. *Nat. Neurosci.* **22**, 1223–1234 (2019).
26. P. Gangopadhyay, M. Chawla, O. Dal Monte, S. W. C. Chang, Prefrontal-amygdala circuits in social decision-making. *Nat. Neurosci.* **24**, 5–18 (2021).

Downloaded at DGIST on November 26, 2021

27. M. G. Baxter, E. A. Murray, The amygdala and reward. *Nat. Rev. Neurosci.* **3**, 563–573 (2002).
28. P. H. Janak, K. M. Tye, From circuits to behaviour in the amygdala. *Nature* **517**, 284–292 (2015).
29. J. J. Kim, M. W. Jung, Neural circuits and mechanisms involved in Pavlovian fear conditioning: A critical review. *Neurosci. Biobehav. Rev.* **30**, 188–202 (2006).
30. J. E. LeDoux, *The Emotional Brain: The Mysterious Underpinnings of Emotional Life* (Simon and Schuster, 1996).
31. S. E. Morrison, C. D. Salzman, Re-valuing the amygdala. *Curr. Opin. Neurobiol.* **20**, 221–230 (2010).
32. P. T. Putnam, K. M. Gothard, Multidimensional neural selectivity in the primate amygdala. *eNeuro* **6**, ENEURO.0153-19.2019 (2019).
33. D. G. Amaral, The amygdala, social behavior, and danger detection. *Ann. N. Y. Acad. Sci.* **1000**, 337–347 (2003).
34. F. Wang, H. W. Kessels, H. Hu, The mouse that roared: Neural mechanisms of social hierarchy. *Trends Neurosci.* **37**, 674–682 (2014).
35. M. E. Walton, D. M. Bannerman, K. Alterescu, M. F. S. Rushworth, Functional specialization within medial frontal cortex of the anterior cingulate for evaluating effort-related decisions. *J. Neurosci.* **23**, 6475–6479 (2003).
36. J. Schweimer, W. Hauber, Involvement of the rat anterior cingulate cortex in control of instrumental responses guided by reward expectancy. *Learn. Mem.* **12**, 334–342 (2005).
37. P. H. Rudebeck, M. E. Walton, A. N. Smyth, D. M. Bannerman, M. F. S. Rushworth, Separate neural pathways process different decision costs. *Nat. Neurosci.* **9**, 1161–1168 (2006).
38. S. B. Floresco, S. Ghods-Sharifi, Amygdala-prefrontal cortical circuitry regulates effort-based decision making. *Cereb. Cortex* **17**, 251–260 (2007).
39. E. Fehr, K. M. Schmidt, A theory of fairness, competition, and cooperation. *Q. J. Econ.* **114**, 817–868 (1999).
40. A. S. Gabay, J. Radua, M. J. Kempton, M. A. Mehta, The Ultimatum Game and the brain: A meta-analysis of neuroimaging studies. *Neurosci. Biobehav. Rev.* **47**, 549–558 (2014).
41. J. Brauer, J. Call, M. Tomasello, Are apes really inequity averse? *Proc. R. Soc. B Biol. Sci.* **273**, 3123–3128 (2006).
42. S. F. Brosnan, F. B. M. De Waal, Monkeys reject unequal pay. *Nature* **425**, 297–299 (2003).
43. K. Jensen, J. Call, M. Tomasello, Chimpanzees are rational maximizers in an ultimatum game. *Science* **318**, 107–109 (2007).
44. M. I. Cordero, C. Sandi, Stress amplifies memory for social hierarchy. *Front. Neurosci.* **1**, 175–184 (2007).
45. L. O. Franco *et al.*, Social subordination induced by early life adversity rewires inhibitory control of the prefrontal cortex via enhanced Npy1r signaling. *Neuropsychopharmacology* **45**, 1438–1447 (2020).
46. Z. Fan *et al.*, Using the tube test to measure social hierarchy in mice. *Nat. Protoc.* **14**, 819–831 (2019).
47. H. Tada *et al.*, Neonatal isolation augments social dominance by altering actin dynamics in the medial prefrontal cortex. *Proc. Natl. Acad. Sci. U.S.A.* **113**, E7097–E7105 (2016).
48. W. Chung *et al.*, Social deficits in IRSp53 mutant mice improved by NMDAR and mGluR5 suppression. *Nat. Neurosci.* **18**, 435–443 (2015).
49. R. R. Holson, Mesial prefrontal cortical lesions and timidity in rats. III. Behavior in a semi-natural environment. *Physiol. Behav.* **37**, 239–247 (1986).
50. E. Lee *et al.*, Enhanced neuronal activity in the medial prefrontal cortex during social approach behavior. *J. Neurosci.* **36**, 6926–6936 (2016).
51. F. Wang *et al.*, Bidirectional control of social hierarchy by synaptic efficacy in medial prefrontal cortex. *Science* **334**, 693–697 (2011).
52. O. Yizhar *et al.*, Neocortical excitation/inhibition balance in information processing and social dysfunction. *Nature* **477**, 171–178 (2011).
53. T. Zhou *et al.*, History of winning remodels thalamo-PFC circuit to reinforce social dominance. *Science* **357**, 162–168 (2017).
54. J. J. Kim, J. W. Koo, H. J. Lee, J. S. Han, Amygdalar inactivation blocks stress-induced impairments in hippocampal long-term potentiation and spatial memory. *J. Neurosci.* **25**, 1532–1539 (2005).
55. B. M. Sharp, Basolateral amygdala and stress-induced hyperexcitability affect motivated behaviors and addiction. *Transl. Psychiatry* **7**, e1194 (2017).
56. A. N. Sciara *et al.*, Neuroinflammatory gene expression alterations in anterior cingulate cortical white and gray matter of males with autism spectrum disorder. *Autism Res.* **13**, 870–884 (2020).
57. R. C. Bagot *et al.*, Circuit-wide transcriptional profiling reveals brain region-specific gene networks regulating depression susceptibility. *Neuron* **90**, 969–983 (2016).
58. Z. S. Lorsch *et al.*, Stress resilience is promoted by a Zfp189-driven transcriptional network in prefrontal cortex. *Nat. Neurosci.* **22**, 1413–1423 (2019).
59. Z. Z. Pan, Transcriptional control of Gad2. *Transcription* **3**, 68–72 (2012).
60. Z. Tan *et al.*, Dynamic ErbB4 activity in hippocampal-prefrontal synchrony and top-down attention in rodents. *Neuron* **98**, 380–393.e4 (2018).
61. R. S. Woo *et al.*, Neuregulin-1 enhances depolarization-induced GABA release. *Neuron* **54**, 599–610 (2007).
62. E. Benito, L. M. Valor, M. Jimenez-Minchan, W. Huber, A. Barco, cAMP response element-binding protein is a primary hub of activity-driven neuronal gene expression. *J. Neurosci.* **31**, 18237–18250 (2011).
63. G. E. Hardingham, Y. Fukunaga, H. Bading, Extrasynaptic NMDARs oppose synaptic NMDARs by triggering CREB shut-off and cell death pathways. *Nat. Neurosci.* **5**, 405–414 (2002).
64. Y. Chen, Y. Wang, Z. Modrusan, M. Sheng, J. S. Kaminker, Regulation of neuronal gene expression and survival by basal NMDA receptor activity: A role for histone deacetylase 4. *J. Neurosci.* **34**, 15327–15339 (2014).
65. S. J. Zhang *et al.*, Decoding NMDA receptor signaling: Identification of genomic programs specifying neuronal survival and death. *Neuron* **53**, 549–562 (2007).
66. C. Bas-Orth, Y. W. Tan, D. Lau, H. Bading, Synaptic activity drives a genomic program that promotes a neuronal Warburg effect. *J. Biol. Chem.* **292**, 5183–5194 (2017).
67. A. C. Janes *et al.*, GABA levels in the dorsal anterior cingulate cortex associated with difficulty ignoring smoking-related cues in tobacco-dependent volunteers. *Neuropsychopharmacology* **38**, 1113–1120 (2013).
68. M. F. Rushworth, M. E. Walton, S. W. Kennerley, D. M. Bannerman, Action sets and decisions in the medial frontal cortex. *Trends Cogn. Sci.* **8**, 410–417 (2004).
69. K. L. Hillman, D. K. Bilkey, Neural encoding of competitive effort in the anterior cingulate cortex. *Nat. Neurosci.* **15**, 1290–1297 (2012).
70. L. P. Baenninger, Social dominance orders in the rat: "Spontaneous" food and water competition. *J. Comp. Physiol. Psychol.* **71**, 202–209 (1970).
71. J. Masur, R. M. Martz, D. Bieniek, F. Korte, Influence of (-) 9 -trans-tetrahydrocannabinol and mescaline on the behavior of rats submitted to food competition situations. *Psychopharmacology (Berl.)* **22**, 187–194 (1971).
72. K. Militzer, H. J. Reinhard, Rank positions in rats and their relations to tissue parameters. *Physiol. Psychol.* **10**, 251–260 (1982).
73. B. Joo, J. W. Koo, S. Lee, Posterior parietal cortex mediates fear renewal in a novel context. *Mol. Brain* **13**, 16 (2020).
74. E. H. Baeg *et al.*, Fast spiking and regular spiking neural correlates of fear conditioning in the medial prefrontal cortex of the rat. *Cereb. Cortex* **11**, 441–451 (2001).
75. L. K. Graham, T. Yoon, J. J. Kim, Stress impairs optimal behavior in a water foraging choice task in rats. *Learn. Mem.* **17**, 1–4 (2009).
76. G. Paxinos, C. Watson, *The Rat Brain in Stereotaxic Coordinates* (Academic Press/Elsevier, Amsterdam, Boston, ed. 6, 2007).
77. S. Andrews, J. Gilley, M. P. Coleman, Difference tracker: ImageJ plugins for fully automated analysis of multiple axonal transport parameters. *J. Neurosci. Methods* **193**, 281–287 (2010).
78. C. Trapnell, L. Pachter, S. L. Salzberg, TopHat: Discovering splice junctions with RNA-Seq. *Bioinformatics* **25**, 1105–1111 (2009).
79. C. Trapnell *et al.*, Transcript assembly and quantification by RNA-Seq reveals unannotated transcripts and isoform switching during cell differentiation. *Nat. Biotechnol.* **28**, 511–515 (2010).
80. C. Trapnell *et al.*, Differential gene and transcript expression analysis of RNA-seq experiments with TopHat and Cufflinks. *Nat. Protoc.* **7**, 562–578 (2012).
81. Y. Benjamini, Y. Hochberg, Controlling the false discovery rate–A practical and powerful approach to multiple testing. *J. R. Stat. Soc. Series B Stat. Methodol.* **57**, 289–300 (1995).
82. W. Huang, B. T. Sherman, R. A. Lempicki, Systematic and integrative analysis of large gene lists using DAVID bioinformatics resources. *Nat. Protoc.* **4**, 44–57 (2009).
83. F. Supek, M. Bošnjak, N. Škunca, T. Šmuc, REVIGO summarizes and visualizes long lists of gene ontology terms. *PLoS One* **6**, e21800 (2011).
84. D. Szklarczyk *et al.*, The STRING database in 2017: Quality-controlled protein-protein association networks, made broadly accessible. *Nucleic Acids Res.* **45**, D362–D368 (2017).
85. P. Shannon *et al.*, Cytoscape: A software environment for integrated models of biomolecular interaction networks. *Genome Res.* **13**, 2498–2504 (2003).
86. J. H. Morris *et al.*, clusterMaker: A multi-algorithm clustering plugin for Cytoscape. *BMC Bioinformatics* **12**, 436 (2011).
87. G. Su, A. Kuchinsky, J. H. Morris, D. J. States, F. Meng, GLay: Community structure analysis of biological networks. *Bioinformatics* **26**, 3135–3137 (2010).
88. J. W. Koo *et al.*, BDNF is a negative modulator of morphine action. *Science* **338**, 124–128 (2012).
89. K. J. Livak, T. D. Schmittgen, Analysis of relative gene expression data using real-time quantitative PCR and the 2(-Delta Delta C(T)) Method. *Methods* **25**, 402–408 (2001).
90. Y. Yang *et al.*, Chromatin remodeling inactivates activity genes and regulates neural coding. *Science* **353**, 300–305 (2016).

Downloaded at DGIST on November 26, 2021